Nucleotide-dependent conformational changes in dynamin: evidence for a mechanochemical molecular spring

Michael H. B. Stowell*†, Bruno Marks*†, Patrick Wigge* and Harvey T. McMahon*‡

*MRC Laboratory of Molecular Biology, Hills Road, Cambridge CB2 2QH, UK
†These authors contributed equally to this work
‡e-mail: hmm@mrc-lmb.cam.ac.uk

The GTPase dynamin plays an essential part in endocytosis by catalysing the fission of nascent clathrin-coated vesicles from the plasma membrane. Using preformed phosphatidylinositol-4,5-bisphosphate-containing lipid nanotubes as a membrane template for dynamin self-assembly, we investigate the conformational changes that arise during GTP hydrolysis by dynamin. Electron microscopy reveals that, in the GTP-bound state, dynamin rings appear to be tightly packed together. After GTP hydrolysis, the spacing between rings increases nearly twofold. When bound to the nanotubes, dynamin's GTPase activity is cooperative and is increased by three orders of magnitude compared with the activity of unbound dynamin. An increase in the k_{cat} (but not the K_m) of GTP hydrolysis accounts for the pronounced cooperativity. These data indicate that a novel, lengthwise ('spring-like') conformational change in a dynamin helix may participate in vesicle fission.

The importance of the dynamin family of high-molecular-weight GTP-binding proteins in membrane traffic has been appreciated for some time[1–4]. The involvement of this family in endocytosis, in particular in the rapid recycling of clathrin-coated vesicles at the *Drosophila* synapse, first became apparent from early studies of the temperature-sensitive mutation dynamin–*shibire*[5–7]. In *shibire* mutants, at the non-permissive temperature, electron microscopy shows the presence of electron-dense rings surrounding deeply invaginated membranes (pits) that are blocked at a late stage of budding. In nerve terminals treated with the non-hydrolysable GTP analogue GTP-γS, endocytosis intermediates are observed that are collared with morphologically similar stacks of electron-dense rings of dynamin[8]. These observations indicate that dynamin rings collaring clathrin-coated pits may be essential in endocytosis. The stacks of dynamin rings observed in these studies appear to be connected as a helix. Experiments in which dominant-negative dynamin constructs were overexpressed in mammalian cells have confirmed the essential function of dynamin in clathrin-mediated endocytosis[9,10].

A major dynamin-binding protein is amphiphysin; this protein is proposed to recruit dynamin to sites of endocytosis by linking it to α-adaptin in the adaptor protein-2 (AP-2) complex[11–13], which is found in clathrin-coated pits. The interaction between dynamin and amphiphysin is inhibited by phosphorylation[14]. When calcium

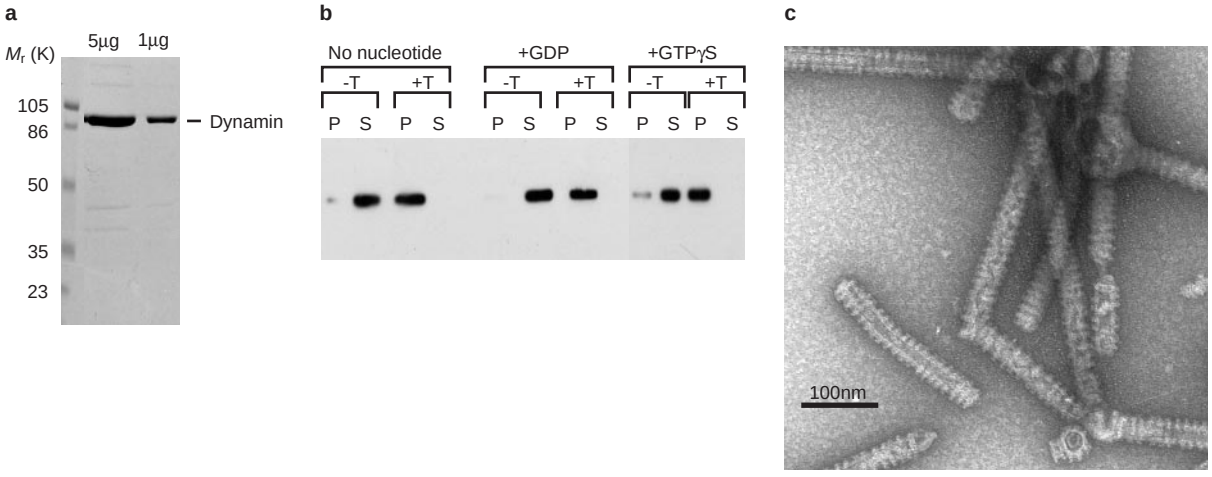

Figure 1 **Purified dynamin associates with lipid nanotubes containing PtdIns(4,5)P_2 and exhibits high GTPase activity. a**, Dynamin purification. Coomassie-stained gel showing 1 μg and 5 μg affinity-purified dynamin (see Methods). **b**, Association of dynamin with PtdIns(4,5)P_2-containing lipid nanotubes under conditions of physiological ionic strength in the presence or absence of 1 mM nucleotides. Purified dynamin was incubated with (+T) or without (–T) lipid nanotubes for 10 min at room temperature, and tubules were pelleted at 60,000*g* to separate associated from non-associated dynamin. Pellets (P) and supernatants (S) were analysed by running on 12% SDS–PAGE gels followed by immunoblotting. **c**, Field view of PtdIns(4,5)P_2 lipid nanotubes decorated with dynamin.

entry into nerves is stimulated by the depolarization of nerve terminals, the phosphatase calcineurin is activated and amphiphysin and dynamin are dephosphorylated, potentially allowing them to interact[13]. Dynamin concentrated at the clathrin-coated pit may be maintained in a non-oligomeric state while bound to amphiphysin[15]. Following recruitment to sites of endocytosis, it is proposed that dynamin redistributes and polymerizes around the vesicle neck. This interaction with the lipid occurs through dynamin's pleckstrin-homology (PH) domain[16,17] which has a specificity for phosphatidylinositols in the membrane[18–21]. Synaptojanin, a lipid 5′ phosphatase[22], could potentially regulate dynamin's affinity for the membrane by modification of the membrane's phosphoinositide composition.

Results of *in vitro* experiments have revealed that dynamin is able to bind and tubulate lipid membranes in the absence of any other accessory factors[23,24]. Dynamin can also catalyse the fission of pure phosphatidylserine tubules by a GTP-dependent reaction, with the minimum components being dynamin, phosphatidylserine vesicles and 1 mM GTP[24]. An important issue concerns the nature of dynamin's conformational change upon GTP hydrolysis. We show here that dynamin's GTPase activity exhibits a distinctive V-type allosteric cooperativity, indicating the potential for concerted activation of a dynamin multimer. Although it has been suggested that the conformational change that occurs is one in which the dynamin rings constrict upon GTP hydrolysis, our results show that the principal conformational change in dynamin is an increase in the pitch of the dynamin helix.

Results

Dynamin associates specifically with PtdIns(4,5)P_2 tubules. As mentioned, dynamin alone will form membrane tubes from lipids to which it can bind. This *in vitro* phenomenon, however, requires high concentrations of dynamin and does not involve its GTPase activity. As our principle aim was to investigate the conformational change in dynamin that is suggested to accompany GTP hydrolysis, we used a preformed lipid template. There is also evidence to suggest that dynamin might not be required to form vesicle necks (or to maintain their stability) *in vivo* (see below).

We prepared lipid nanotubes, which are similar in size to the constricted necks of clathrin-coated pits observed *in vivo*[8,25], from a mixture of non-hydroxylated fatty-acid galactoceramides (NFA-GalCer), phosphatidylcholine, cholesterol, and phosphatidylinositol-4,5-bisphosphate (PtdIns(4,5)P_2). The relative proportions of each lipid approximated the composition of synaptic vesicles[26], but with increased concentrations of NFA-GalCer, which promotes the formation of a tubular lipid structure rather than vesicles. Phosphoinositides interact with dynamin's PH domain and activate dynamin's GTPase activity; PtdIns(4,5)P_2 is the best such activator[18,20,21,27] and we therefore included PtdIns(4,5)P_2 and refer

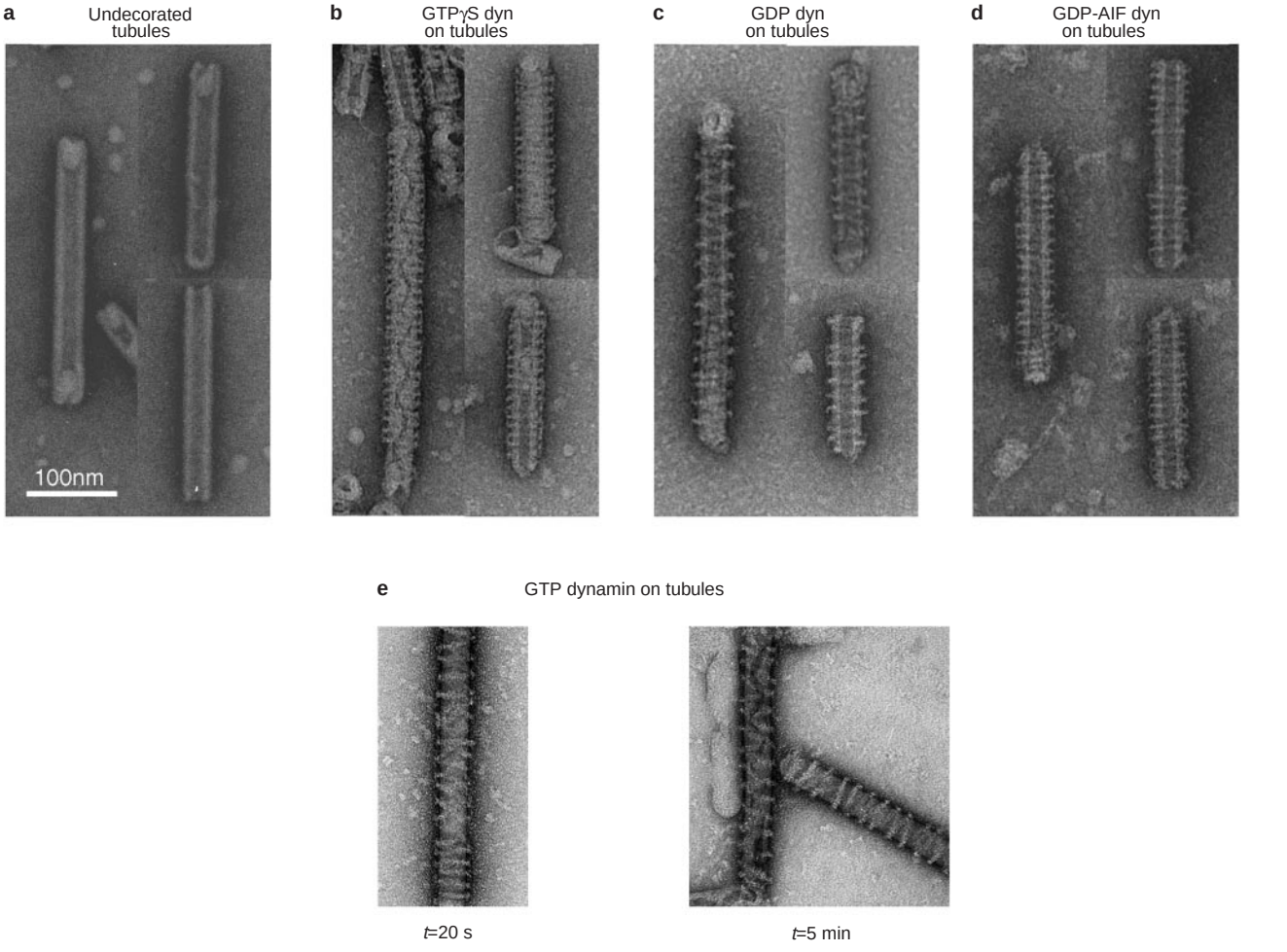

Figure 2 **The conformational states of dynamin in the presence of different nucleotides.** Tubules were prepared for negative-stain electron microscopy, in the presence of 0.5 μM dynamin and 1 mM of different nucleotides. In **e**, *t*=20 s represents the shortest time point measurable. At this time point GTP is being rapidly hydrolysed.

to these tubes as 'PtdIns(4,5)P_2 nanotubes'.

We incubated rat brain dynamin, affinity-purified using the Src-homology-3 (SH3) domain of amphiphysin-2 (Fig. 1a), with PtdIns(4,5)P_2 nanotubes in buffer of physiological ionic strength (160 mM), and measured binding by a co-sedimentation assay. Only in the presence of nanotubes was dynamin pelleted effi ciently and this process occurred in a nucleotide-independent manner (Fig. 1b). Electron microscopy showed that the pelleting was due to the binding of the dynamin to the lipid nanotubes to give a high-order oligomer in the form of stacks of rings resembling a helix (Fig. 1c).

GTP- and GDP-bound dynamin adopt distinct conformations. We studied dynamin-coated nanotubes in the presence of various nucleotides by electron microscopy. PtdIns(4,5)P_2 lipid nanotubes prepared in the absence of dynamin are shown in Fig. 2a. When such nanotubes were incubated with dynamin (0.5 μM) in the presence of 100–1,000 μM GTP-γS, dynamin assembled into highly ordered and tightly packed stacks of rings (Fig. 2b). The rings usually appeared to sit obliquely about the tubules, suggesting that they form a continuous helix having a pitch (inter-ring spacing) of 11±1.5 nm, with outer and inner diameters of 32±1 nm and 40±1.5 nm, respectively. Dynamin assembled in the presence of GDP plus aluminium fluoride, which mimics the nucleotide's transition state[28,29], also exhibited a well-ordered, tightly packed conformation, with similar dimensions to the dynamin assembled in the presence of GTP-γS (Fig. 2d).

Dynamin-GDP, in contrast, showed a very different helical conformation. Although both the inner and the outer diameters of the dynamin tubules were unchanged (outer and inner diameters of 32±2 nm and 40±2.5 nm, respectively), the helix became much more uncoiled, with a dramatic increase in pitch to 20±3 nm (Fig. 2c). In this GDP-bound conformation, a right-handed helical appearance was particularly evident. This conformation was most apparent at a GDP concentration of 1 mM, consistent with a low affinity of dynamin for GDP[30]. Below this GDP concentration, much of the dynamin was in a loose but more disordered state, with variable pitch between rings.

We also observed nucleotide-specific dynamin conformations on lipid nanotubes made with total brain lipid extract (Folsch fraction I) supplemented with NFA-GalCer (data not shown). Dynamin incubated with GTP in the absence of magnesium oligomerized on PtdIns(4,5)P_2-containing nanotubes in a similar conformation to that of dynamin incubated with low GDP concentrations. Shortly after the addition of $MgCl_2$, tubes often had short stretches of GTPgS-like dynamin (tightly packed) amidst dynamin in looser spirals (Fig. 2e). After longer incubation times, the dynamin returned again to being almost exclusively in the 'loose' state (pitch 19±3 nm). All measurements of nucleotide-specific conformations are averaged from multiple electron micrographs from at least three different experiments for each condition.

Dynamin's GTPase activity increases on binding to lipid tubules. These results indicate that dynamin's principal conformational change is an increase in pitch upon GTP hydrolysis — a lengthwise helical expansion. If the force generated by this mechanism is to break the lipid tubule, it would ideally be applied in a rapid and concerted fashion that would allow less energy to be absorbed by lipid deformation than would a slow expansion. We therefore studied the kinetic properties of the dynamin GTPase to determine whether they concur with this ideal scenario.

We performed GTPase assays under the same buffer conditions as those used for the structural observations; most important, we maintained a physiological ionic strength of 160 mM. PtdIns(4,5)P_2 tubules supported a high rate of GTP hydrolysis by dynamin, and their disruption with Triton-X100 abolished this effect (Fig. 3a, b). Dynamin alone, or in the presence of lipid nanotubes lacking PtdIns(4,5)P_2, showed negligible GTPase activity (Fig. 3b). In addition, a recently characterized dynamin PH-domain mutant, K535A, which is unable to bind to lipid membranes and inhibits endocytosis[16,17], was not stimulated by PtdIns(4,5)P_2 tubules. These results show that, under physiological ionic conditions, the ability of dynamin to bind to a suitable template is essential for its oligomerization and consequent increased GTPase activity. A calculation of initial rates of GTP hydrolysis from Fig. 3b shows that the activation by PtdIns(4,5)P_2 tubules is roughly 1,000-fold (as compared to the rate of GTP hydrolysis by dynamin alone). This is the highest degree of activation measured for dynamin's GTPase activity under physiological ionic-strength conditions. Previous work has identified several other potential activators of GTP hydrolysis[21,27,30–33], but all resulted in relatively modest (10–50-fold) rates of activation.

V-type allostery underlies dynamin's cooperativity. Previous studies, using conditions of low ionic strength, have shown a cooperative activation of dynamin's GTPase activity, although the kinetic nature of this activation was not determined[32,34–36]. We observed that dynamin's PtdIns(4,5)P_2-tubule-associated GTPase activity shows a striking concentration dependence (Fig. 4b). To establish the precise nature of this effect, we measured initial rates of GTP hydrolysis at various GTP and dynamin concentrations (Fig. 4a) and determined the kinetic parameters K_m and k_{cat}. Over the dynamin concentration range studied, there was no significant change in K_m (Fig. 4d). The observed value (15±3.7 μM at 1.0 μM dynamin) was in good agreement with previous measurements[30] and well below physiological concentrations of GTP (50–150 μM)[37]. In contrast, we found a significant (>15-fold) increase in the apparent k_{cat} from 0.3 s^{-1} to 4.6 s^{-1} (Fig. 4c, d). Thus, dynamin shows V-type allostery[38], whereby its enzymatic efficiency rises as the equilibrium is shifted from an inactive to an active multimeric form of dynamin. This is a rarely observed characteristic and contrasts with the more commonly observed and far better understood K-type allostery, in which substrate-binding

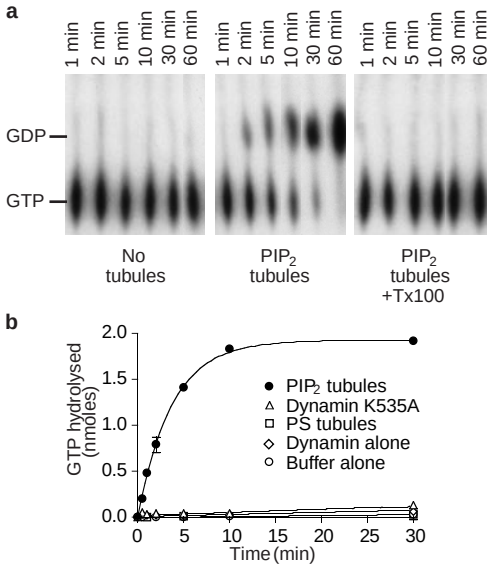

Figure 3 **High rates of GTP hydrolysis by tubule-associated dynamin. a**, GTPase activity of dynamin on PtdIns(4,5)P_2 (PIP_2) tubules. Shown is an example of an autoradiogram obtained from a typical GTPase assay carried out by separation of ^{32}P-labelled guanine nucleotides using thin-layer chromatography. Solubilization of tubules with 0.1% Triton-X100 (Tx100) abolished this activation. **b**, Quantification of dynamin's GTPase activation on PtdIns(4,5)P_2 tubules. Levels of GTP hydrolysis in the presence of PtdIns(4,5)P_2 or phosphatidylserine (PS) tubules (~50 μM lipid) were measured on a phosphorimager using ImageQuant software. A comparison of initial rates of hydrolysis reveals a >1,000-fold rate of activation of GTP hydrolysis by PtdIns(4,5)P_2 tubules, compared with the rate of GTP hydrolysis by dynamin alone. Results are the average of three experiments ±s.e.m.

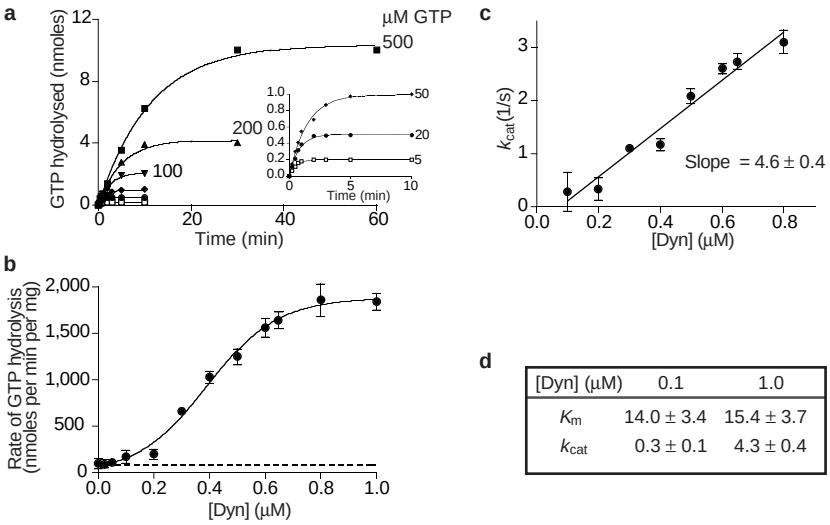

d

[Dyn] (μM)	0.1	1.0
K_m	14.0 ± 3.4	15.4 ± 3.7
k_{cat}	0.3 ± 0.1	4.3 ± 0.4

Figure 4 **Cooperativity and V-type allostery of dynamin's GTPase activity. a**, Typical raw kinetic data from which the catalytic constants K_m and k_{cat} were derived. Dynamin (0.5 μM) and PtdIns(4,5)P_2 tubules (100 μM, 10% PtdIns(4,5)P_2) were preincubated for 10 min before initiation of GTPase assays by the addition of GTP to final concentrations between 5 and 500 μM. **b**, Increasing dynamin concentration increases the extent of GTPase activation by PtdIns(4,5)P_2 tubules in a cooperative fashion. GTPase assays were performed at a fixed GTP concentration of 100 μM, and a dynamin concentration ranging from 0.05 to 1.0 μM. **c**, **d**, The cooperativity of dynamin's GTPase activity is due to an increase in k_{cat} and not a change in its substrate-binding affinity, K_m. Values were determined from a series of GTPase assays, as shown in **a**, done in the presence of 5–500 μM GTP and varying concentrations of dynamin.

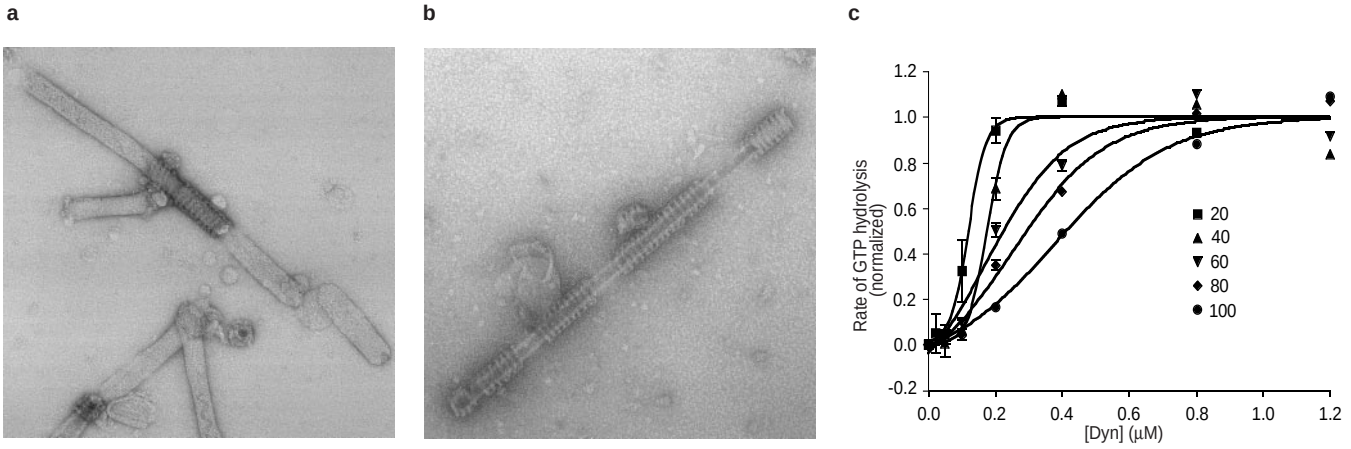

Figure 5 **Potential involvement of stacks of rings in optimal GTP hydrolysis. a**, **b**, Visualization of dynamin structures under different dynamin:tubule ratios. Dynamin is always observed to form stacks of rings (and not single rings) even at low concentrations (**a**). Dynamin concentrations used were 0.1 μM (**a**) and 0.25 μM (**b**), both in the presence of 100 μM GTP-γS and 500 μM lipid. **c**, Effect of dynamin:tubule (total lipid) ratio on dynamin cooperativity. As this ratio is decreased (that is, the amount of dynamin per tubule decreases), the specific activity of dynamin also decreases. As the tubule concentration is increased, the dynamin concentration has to be increased to maintain a given level of GTPase activity. The total lipid concentration (in μM) is indicated by symbols. In all cases, the PtdIns(4,5)P_2 concentration was maintained at 10%.

affinity is improved in the cooperative state.

Involvement of stacks of rings in cooperative GTPase activity. At low concentrations of dynamin (0.1 μM), most of the lipid nanotubes lacked dynamin and the remaining tubules typically had single short stacks (Fig. 5a). Single rings were rarely observed, even at the lowest concentration of dynamin studied. As the concentration of dynamin was increased, the number of stacks per tubule and the number of rings per stack increased (Fig. 5b). At the highest concentrations studied, the lipid nanotubes appeared to be completely covered with dynamin rings. The minimum concentration at which significant dynamin GTPase activity was measurable (~0.1–0.2 μM) corresponded to the concentration at which stacks became observable (Fig. 5a).

To investigate the importance of the dynamin stacks further, we measured GTPase activity under different dynamin:tubule (total lipid) ratios (Fig. 5c). An excess of tubules led to a shift in the enzyme cooperativity curve, such that higher concentrations of dynamin were required to maintain the same level of activity as obtained when tubules were limiting. Thus, the addition of excess tubules appeared to result in a 'dilution' of the cooperative state of dynamin. This could be explained by the dispersal of long dynamin stacks into shorter multimers.

When dynamin forms multi-ringed oligomers around a lipid tubule there is the potential for two types of interaction between dynamin molecules. First, interactions might occur between adjacent dynamins within the same ring; these interactions would be present in a single ring oligomer; and second, interactions might take place along the longitudinal axis of the tubule between

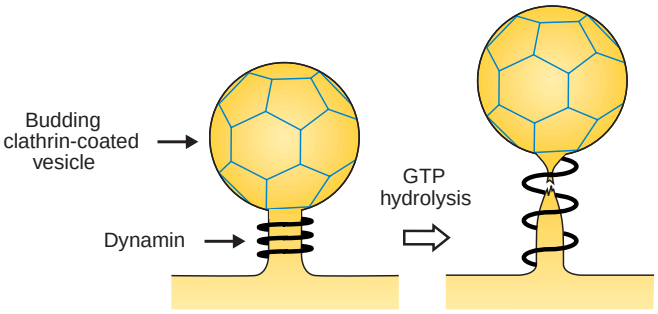

Figure 6 **Model for a concerted helical expansion that drives endocytosis.** Dynamin is recruited to the neck of a budding vesicle, binds GTP and assumes a compressed helical state. Following the concerted hydrolysis of GTP, the dynamin spring extends, shearing the lipid neck at the region of least stability, most likely nearest the clathrin coat.

dynamin molecules occupying corresponding positions in adjacent rings. Our data indicate that this second type of interaction may be important in the activation of dynamin's GTPase activity.

Discussion

We have studied the molecular consequences of GTP hydrolysis by dynamin using preformed lipid nanotubes of defined composition as a template for dynamin oligomerization. Our data are, to our knowledge, the first to show a relationship between dynamin's conformation and its nucleotide-bound state.

The marked change from tightly packed dynamin stacks in the GTP-bound state to a more loose, 'uncoiled' structure in the GDP-bound state indicates a way in which nucleotide hydrolysis by dynamin might result in the generation of a lengthwise force that would destabilize a nascent vesicle neck sufficiently to sever it (Fig. 6). The fact that vesiculation was not observed in any of our experiments suggests that, during GTP hydrolysis, dynamin rings may simply slide over the lipid tubule. Conditions *in vivo*, such as the presence of a barrier at each end against which to 'push' (the clathrin-coated vesicle at one end and the plasma membrane at the other), may be necessary to achieve membrane fission. Also, *in vivo*, the aperture of the clathrin cage, through which the lipid tubule must be connected to the nascent vesicle, appears to produce a potential point of weakness in the membrane, because of the diameter restriction (the internal diameter of a clathrin hexagon is ~24 nm (refs 39,40) and high degree of lipid curvature.

Dynamin's allosteric kinetics fit well with a model in which several dynamin rings would form around a vesicle neck before significant GTPase activation could occur. Once above a threshold level of multimerization, GTP hydrolysis would become rapid and concerted, producing the conformational change necessary for fission. It is important to ask whether or not such a mechanism is energetically feasible. The failure energies of a typical lipid system under tensile stress have been measured[41], and range from 20 to 190 J mol^{-1}, with a force constant (stress) between 0.01 and 0.03 N m^{-1}. The concerted hydrolysis of 60 GTPs (we estimate the number of dynamins per ring to be roughly 20, on the basis of the average size of a protein of relative molecular mass 100,000 and assuming a monomeric state; thus 60 GTP-binding sites correspond to about three turns of the dynamin helix) would give maximally 5×10^{-18} J (3,000 J mol^{-1}) of work. Application of Hooke's law (work = $0.5 \times Kx^2$, where K is the spring force constant and x is the displacement) gives a spring force constant of 0.011 N m^{-1}, comparative to the value of ref. 41. This equates to 330 pN per three-turn helix of dynamin or 5.5 pN of force per dynamin molecule. As an interesting comparison, the force generated by kinesin has been measured (using laser tweezers) at 6 pN per ATP hydrolysed[42]. In future experiments we hope to measure the force generated by dynamin similarly.

Dynamin is capable of tubulating liposomes under certain *in vitro* conditions[23,24] and we have confirmed this (data not shown). However, some observations argue against this being an essential function of dynamin *in vivo*. Deeply invaginated, coated-pit profiles are still observed in lamprey nerve terminals in which dynamin recruitment is thought to have been blocked[13]. It has also been shown *in vitro* that a clathrin-coat fraction can deform lipids into coated vesicles in the absence of dynamin[23]. This would necessarily define the maximum diameter of a vesicle neck as that of an aperture in the clathrin-cage structure (see above). Another protein involved in endocytosis — amphiphysin — is also capable of tubulating lipids *in vitro*[43] and there are also examples of proteins of otherwise unrelated function that can do the same[44]. In view of these observations (and others), there appears to be insufficient evidence, at present, to conclude that dynamin is essential for lipid tubulation *in vivo*.

Although we were unable to observe fission in our model system, it has been observed under different conditions *in vitro*[24]. Recent theoretical modelling (M. M. Kozlov, personal communication) based on published observations[24] combined with accepted models of membrane dynamics shows that the most likely conformational change in dynamin that would result in fission is a lengthwise expansion of a dynamin helix, resulting in a moderate tightening and significant destabilization of the lipid tubule within. In the *in vitro* fission reported[24], the observation that the diameter of the resulting vesicles can be larger than that of the precursor tubules (50 nm average) is a factor that argues against a previous hypothesis postulating that it is purely a constriction of individual dynamin rings that is the conformational change responsible for fission [2,45]. Such a mechanism would be expected to give vesicles of a diameter smaller than that of their precursor.

The results of the mentioned theoretical study (M. M. Kozlov, personal communication) are in agreement with our experimental observations and our nanospring model for dynamin action. Dynamin is frequently referred to as a 'pinchase'; however, our results indicate that the term 'poppase' might be more appropriate.

Methods

Preparation of lipid nanotubes.

Lipid nanotubes were prepared by a modification of the procedure described in ref. 46: we omitted the dimethylformamide and instead extruded the lipids through a filter with pore sizes of 0.2 µm. The lipid composition was 40% phosphatidylcholine, 40% NFA-GalCer, 10% cholesterol and 10% PtdIns(4,5)P_2. Where phosphatidylinositol or phosphatidylserine was substituted for PtdIns(4,5)P_2, we used higher percentages of these lipids than of PtdIns(4,5)P_2 to maintain the charge ratio (the proportion of phosphatidylcholine being reduced accordingly). This method gave tubules of average diameter 28 nm (there was little variation of tubule diameter within or between tubules) and average length 500 nm.

Purification of rat brain dynamin.

Dynamin was purified from rat brain using a recombinant amphiphysin-2 SH3 domain as an affinity ligand. Brain extracts were prepared as described[47], and incubated with 10 mg ml^{-1} glutathione-*S*-transferase-tagged amphiphysin-2 SH3 domain on glutathione–agarose beads at 4 °C. After extensive washing of the matrix in buffer A (200 mM NaCl, 20 mM HEPES, pH 7.3, 1 mM dithiothreitol (DTT)), dynamin was eluted in 3 ml buffer B (1.2 M NaCl, 20 mM PIPES, pH 6.5, 1mM DTT), and dialysed overnight into 100 mM NaCl, 20 mM HEPES, 50% glycerol. Purified dynamin was a mixture of the 94K and 96K splice forms[35] and determined to be >95% pure by coomassie gel analysis. Protein was quantified by the BCA assay (Pierce). K535A mutant dynamin[16] was purified as above from COS-7 fibroblasts overexpressing this protein.

Dynamin multimerization assay.

Dynamin assembly on tubules was monitored either by electron microscopy or using a spin assay, in which assembled dynamin can be pelleted by centrifugation at 60,000*g* for 15 min and analysed by SDS–PAGE followed by immunoblotting. Assembly was carried out in a 50 µl reaction volume under identical conditions to those used for GTP hydrolysis, with 0.5 µM dynamin and 1 mM nucleotide, and incubated at room temperature for 5–10 min.

Dynamin GTPase assay.

All GTPase assays were done at room temperature. Tubules (0.1 mM lipid) and dynamin (typically 0.5 µM) were incubated for 10 min at room temperature in buffer C (135 mM NaCl, 5 mM KCl, 20 mM HEPES, pH 7.4, 1 mM $MgCl_2$) and then reactions (in 20 µl) were initiated by the addition of GTP (normally to 100 µM) and 10 µCi ml^{-1} [α-^{32}P]GTP. GTP hydrolysis was analysed by thin-layer chromatogra-

phy on PEI cellulose (Sigma) and results were quantified using a phosphorimager and ImageQuant software (Molecular Dynamics). Raw kinetic data were transferred to the GraphPad suite of kinetic analysis programs. Lineweaver–Burk analysis of data allowed us to determine the K_m and k_{cat} (V_{max}/[Dyn]) at various dynamin concentrations.

Electron microscopy.

Samples for microscopy were prepared by mixing lipid nanotubes, dynamin and various nucleotides together and incubating them at room temperature for 10 min. Carbon-coated 350-mesh grids were glow-discharged and subsequently samples were applied and blotted. Samples were stained with 0.5% uranyl acetate and imaged on a Phillips 208 80-kV electron microscope. Images were recorded at a magnification of ×63,000 and digitized using a Zeiss SCIA scanner using 21-micron pixel digitization.

RECEIVED 24 FEBRUARY 1999; REVISED 12 MARCH 1999; ACCEPTED 12 MARCH 1999; PUBLISHED MAY 1999.

1. Roos, J. & Kelly, R. B. Is dynamin really a 'pinchase'? *Trends Cell Biol.* **7,** 257–259 (1997).
2. McNiven, M. A. Dynamin: a molecular motor with pinchase action. *Cell* **94,** 151–154 (1998).
3. Schmid, S. L. Clathrin-coated vesicle formation and protein sorting: an integrated process. *Annu. Rev. Biochem.* **66,** 511–548 (1997).
4. DeCamilli, P. & Takei, K. Molecular mechanisms in synaptic vesicle endocytosis and recycling. *Neuron* **16,** 481–486 (1996).
5. Poodry, C. A. & Edgar, L. Reversible alterations in the neuromuscular junctions of *Drosophila melanogaster* bearing a temperature-sensitive mutation, *shibire*. *J. Cell Biol.* **81,** 520–527 (1979).
6. Koenig, J. H. & Ikeda, K. Disappearance and reformation of synaptic vesicle membrane upon transmitter release observed under reversible blockage of membrane retrieval. *J. Neurosci.* **9,** 3844–3860 (1989).
7. Ramaswami, M., Krishnan, K. S. & Kelly, R. B. Intermediates in synaptic vesicle recycling revealed by optical imaging of *Drosophila* neuromuscular junctions. *Neuron* **13,** 363–375 (1994).
8. Takei, K., McPherson, P. S., Schmid, S. L. & DeCamilli, P. Tubular membrane invaginations coated by dynamin rings are induced by GTPγS in nerve terminals. *Nature* **374,** 186–190 (1995).
9. Herskovits, J. S., Burgess, C. C., Obar, R. A. & Vallee, R. B. Effects of mutant rat dynamin on endocytosis. *J. Cell Biol.* **122,** 565–578 (1993).
10. van der Bliek, A. M. *et al.* Mutations in human dynamin block an intermediate stage in coated vesicle formation. *J. Cell Biol.* **122,** 553–563 (1993).
11. Wigge, P. & McMahon, H. T. The amphiphysin family of proteins and their role in endocytosis at the synapse. *Trends Neurosci.* **21,** 339–344 (1998).
12. Shupliakov, O. *et al.* Synaptic vesicle endocytosis impaired by disruption of dynamin-SH3 domain interactions. *Science* **276,** 259–263 (1997).
13. Marks, B. & McMahon, H. T. Calcium triggers calcineurin-dependent synaptic vesicle recycling in mammalian nerve terminals. *Curr. Biol.* **8,** 740–749 (1998).
14. Slepnev, V. I., Ochoa, G. C., Butler, M. H., Grabs, D. & DeCamilli, P. Role of phosphorylation in regulation of the assembly of endocytic coat complexes. *Science* **281,** 821–824 (1998).
15. Owen, D. J. *et al.* Crystal structure of the Amphiphysin-2 SH3 domain and its role in prevention of dynamin ring formation. *EMBO J.* **17,** 5273–5285 (1998).
16. Vallis, Y., Wigge, P., Marks, B., Evans, P. R. & McMahon, H. T. Importance of the pleckstrin homology domain of dynamin in clathrin-mediated endocytosis. *Curr. Biol.* **9**, 257–260 (1999).
17. Achiriloaie, M., Barylko, B. & Albanesi, J. P. Essential role of the dynamin pleckstrin homology domain in receptor mediated endocytosis. *Mol. Cell. Biol.* **19**, 1410–1415 (1999).
18. Zheng, J. *et al.* Identification of the binding site for acidic phospholipids on the pH domain of dynamin: implications for stimulation of GTPase activity. *J. Mol. Biol.* **255,** 14–21 (1996).
19. Salim, K. *et al.* Distinct specificity in the recognition of phosphoinositides by the pleckstrin homology domains of dynamin and Bruton's tyrosine kinase. *EMBO J.* **15,** 6241–6250 (1996).
20. Klein, D. E., Lee, A., Frank, D. W., Marks, M. S. & Lemmon, M. A. The pleckstrin homology domains of dynamin isoforms require oligomerization for high affinity phosphoinositide binding. *J. Biol. Chem.* **273,** 27725–27733 (1998).
21. Barylko, B. *et al.* Synergistic activation of dynamin GTPase by Grb2 and phosphoinositides. *J. Biol. Chem.* **273,** 3791–3797 (1998).
22. McPherson, P.S. *et al.* A presynaptic inositol-5-phosphatase. *Nature* **379,** 353–357 (1996).
23. Takei, K. *et al.* Generation of coated intermediates of clathrin-mediated endocytosis on protein-free liposomes. *Cell* **94,** 131–141 (1998).
24. Sweitzer, S. M. & Hinshaw, J. E. Dynamin undergoes a GTP-dependent conformational change causing vesiculation. *Cell* **93,** 1021–1029 (1998).
25. Koenig, J. H. & Ikeda, K. Synaptic vesicles have two distinct recycling pathways. *J. Cell Biol.* **135,** 797–808 (1996).
26. Deutsch, J. W. & Kelly, R. B. Lipids of synaptic vesicles: relevance to the mechanism of membrane fusion. *Biochemistry* **20,** 378–385 (1981).
27. Tuma, P. L., Stachniak, M. C. & Collins, C. A. Activation of dynamin GTPase by acidic phospholipids and endogenous rat brain vesicles. *J. Biol. Chem.* **268,** 17240–17246 (1993).
28. Steinweis, P. C. & Gilman, A. G. Aluminium: a requirement for activation of the regulatory component of adenylate cyclase by fluoride. *Proc. Natl Acad. Sci. USA* **79,** 4888–4891 (1982).
29. Carr, J. F. & Hinshaw, J. E. Dynamin assembles into spirals under physiological salt conditions upon the addition of GDP and gamma-phosphate analogues. *J. Biol. Chem.* **272,** 28030–28035 (1997).
30. Shpetner, H. S. & Vallee, R. B. Dynamin is a GTPase stimulated to high levels of activity by microtubules. *Nature* **355,** 733–735 (1992).
31. Gout, I. *et al.* The GTPase dynamin binds to and is activated by a subset of SH3 domains. *Cell* **75,** 25–36 (1993).
32. Herskovits, J. S., Shpetner, H. S., Burgess, C. C. & Vallee, R. B. Microtubules and src homology 3 domains stimulate the dynamin GTPase via its C-terminal domain. *Proc. Natl Acad. Sci. USA* **90,** 11468–11472 (1993).
33. Robinson, P. J. *et al.* Dynamin GTPase regulated by protein kinase C phosphorylation in nerve terminals. *Nature* **365,** 107–108 (1993).
34. Tuma, P. L. & Collins, C. A. Activation of dynamin GTPase is a result of positive cooperativity. *J. Biol. Chem.* **269,** 30842–30847 (1994).
35. Warnock, D. E., Hinshaw, J. E. & Schmid, S. L. Dynamin self-assembly stimulates its GTPase activity. *J. Biol. Chem.* **271,** 22310–22314 (1996).
36. Shpetner, H. S. & Vallee, R. B. Identification of dynamin, a novel mechanochemical enzyme that mediates interactions among microtubules. *Cell* **59,** 421–432 (1989).
37. Otero, A. D. Transphosphorylation and G protein activation. *Biochem. Pharmacol.* **39,** 1399–1404 (1990).
38. Monod, J., Wyman, J. & Changeux, J.-P. On the nature of allosteric transitions: a plausible model. *J. Mol. Biol.* **12,** 88–118 (1965).
39. Smith, C. J., Grigorieff, N. & Pearse, B. M. Clathrin coats at 21 Å resolution: a cellular assembly designed to recycle multiple membrane receptors. *EMBO J.* **17,** 4943–4953 (1998).
40. Heuser, J. E. The role of coated vesicles in recycling of synaptic vesicle membrane. *Cell Biol. Int. Report* **13,** 1063–1076 (1989).
41. Needham, D. & Nunn, R. S. Elastic deformation and failure of lipid bilayer membranes containing cholesterol. *Biophys. J.* **58,** 997–1009 (1990).
42. Block, S. M. Nanometers and piconewtons — the macromolecular mechanics of kinesin. *Trends Cell Biol.* **5,** 169 (1995).
43. Takei, K., Slepnev, V. I., Hauck, V. & De Camilli, P. Amphiphysin tubulates protein free liposomes and regulates the formation of clathrin- and dynamin- coated structures *in vitro*. *Mol. Biol. Cell Abstr.* **9-S,** 130 (1998).
44. Polyakov, A., Severinova, E. & Darst, S. A. Three dimensional structure of *E. coli* core RNA polymerase: promoter binding and elongation conformations of the enzyme. *Cell* **83,** 365–373 (1995).
45. Warnock, D. E. & Schmid, S. L. Dynamin GTPase, a force-generating molecular switch. *Bioessays* **18,** 885–894 (1996).
46. Goldstein, A. S., Lukyanov, A. N., Carlson, P. A., Yager, P. & Gelb, M. H. Formation of high-axial-ratio-microstructures from natural and synthetic sphingolipids. *Chem. Phys. Lipids* **88,** 21–36 (1997).
47. Wigge, P. *et al.* Amphiphysin heterodimers: potential role in clathrin-mediated endocytosis. *Mol. Biol. Cell* **8,** 2003–2015 (1997).

ACKNOWLEDGEMENTS

We thank M. M. Kozlov for discussions and providing unpublished data, and N. Unwin for encouragement and discussions. This work was supported by the MRC and an NSF-NATO Postdoctoral Fellowship (M.H.B.S.).

Correspondence and requests for materials should be addressed to H.T.M.